The site and pseudodonor character of manganese in single-crystal lead telluride

1990 J. Phys.: Condens. Matter 2 10391

(http://iopscience.iop.org/0953-8984/2/51/012)

J. Phys.: Condens. Matter 2 (1990) 10391–10400. Printed in the UK

The site and pseudodonor character of manganese in single-crystal lead telluride

Yu S Gromovoj, S V Plyatsko, F F Sizov and L A Korovina
Institute of Semiconductors, Ukrainian SSR, PR Nauki 45, Kiev 252650, USSR

Received 10 October 1989, in final form 9 July 1990

Abstract. From the analysis of electron paramagnetic resonance (EPR) spectra and the electrical characteristics of as-grown, long-period 'annealed' at room temperature and laser annealed PbTe:Mn single crystals with Mn content $N_{MN} \simeq 2\text{–}7 \times 10^{18}\,cm^{-3}$ we infer that Mn^{2+} ions in as-grown crystals are incorporated partly interstitially and partly in the metal sublattice sites. In crystals with $N_{Mn} \geqslant 2 \times 10^{19}\,cm^{-3}$ Mn ions tend to form clusters. In such cases manganese behaves as an amphoteric impurity, as a small amount of Mn ions in the metal sublattice points cannot compensate for the large number of Pb vacancies ($N_{Pb} \sim 5 \times 10^{19}\,cm^{-3}$) that act as acceptors. When creating the conditions that promote migration of Mn ions into PbTe metal sublattice points (long-period 'annealing' at $T =$ 300 K, IR laser annealing) which is tested by hyperfine structure and superhyperfine structure of EPR spectra, the Mn^{2+} ions act as pseudodonors, compensating for two holes from each lead vacancy. The electron concentration in such a case is attributed to Te vacancies, which are donors. The spin-Hamiltonian constants were determined at $T = 20$ K for as-grown, long-period 'annealed' and laser annealed PbTe:Mn crystals.

1. Introduction

The position of impurities in IV–VI narrow-gap semiconductor lattices is of importance both from the point of view of the nature of the impurity states, which as a rule one may treat as deep states [1], and also from the point of view of alloying mechanisms, which are not yet clear enough for these substances. For example, one can mention the behaviour of group III elements in PbTe-like semiconductors [1, 2] where their charge states and position in the lattice are not yet well established (see also [3–5]).

Here, the position of Mn impurity and its alloying mechanism in PbTe single crystals with different Mn content, both as-grown and subjected to additional treatments, was investigated by electron paramagnetic resonance (EPR). Electrical, photoelectrical and optical transmission measurements of these crystals were also used.

Establishing the nature of the paramagnetic impurities positions in IV–VI semiconductors and development of the methods of their purposeful installation into the lattice points seem to be very important from the point of view of the nature of the electronic and semimagnetic properties of these objects. Apparently until now only PbTe single crystals containing predominantly Mn clusters have been investigated. The distribution and position of magnetic impurities in the lattice of semimagnetic semiconductors will inevitably strongly affect the electronic and semimagnetic properties of these crystals.

0953-8984/90/5110391 + 10 $03.50

EPR measurements of EPR active centres seems to be convenient in obtaining information on the charge states and position of impurities and their changes in IV–VI semiconductors under different kinds of treatments [6, 7].

For example, it was shown in [7] that in as-grown PbTe crystals Eu impurities form clusters that decompose under infra-red (IR) laser treatment. After such treatment the Eu ions are in metal-sublattice points. In [6] it was shown that in Mn ion doped PbTe epitaxial layers, subjected to thermal treatment at $T \leqslant 340$ °C, the Mn ions are in metallic sublattice points too. But at thermal treatment temperatures, $T > 370$ °C, the Mn-impurity tends to cluster.

Manganese is the most widely studied EPR active impurity in IV–VI semiconductors. In earlier papers devoted to the investigation of the EPR spectra in PbTe : Mn crystals [8–13] only six lines of hyperfine interaction or one broad line were revealed in EPR spectra which did not give the opportunity to identify the location of Mn ions in the lead telluride lattice. Moreover, another six lines of hyperfine structure (HFS) in some PbTe : Mn single crystals were revealed near the 'ordinary' six lines of HFS [13]. In [12] an additional six lines were also revealed but in $Pb_{1-x}Sn_xTe$ solid solution crystals. The authors explain this fact by the inhomogeneous distribution of Pb and Sn atoms.

Superhyperfine structure (SHFS) in the EPR spectra of Mn^{2+}, giving the opportunity to confirm Mn^{2+} Pb's sublattice position in the lead telluride lattice, was recently observed in PbTe single crystals doped with Mn in small amounts ('traces' of Mn) [14]. But these results do not permit the identification of the position of Mn ions in PbTe crystals with large Mn content (in so-called semimagnetic (diluted magnetic semiconductors) crystals—in this case—$Pb_{1-x}Mn_xTe$ crystals).

SHFS of Mn^{2+} ions interacting with Te nuclei of the first coordinate sphere was also recently revealed in PbTe epitaxial layers (on BaF_2 substrates) [6], annealed at temperatures $T \leqslant 340$ °C. Higher annealing temperatures, that one ordinarily uses for crystal and epitaxial layer growth, lead to the disappearance of SHFS, caused by clustering of Mn [6].

Clustering of Mn impurities has been postulated in $Pb_{1-x}Mn_xTe$ single crystals grown from the melt [12, 15, 16]. From the quantitative analysis of magnetic susceptibility measurements [16] it was concluded that the effective Mn concentration is much smaller than the incorporated one. In [17], also from the analysis of magnetic susceptibility measurements, it was inferred that Mn clustering begins from $N_{Mn} \simeq 2 \times 10^{19}$ cm^{-3} (in Czochralsky grown crystals).

Under ordinary methods of doping, manganese manifests its amphoteric character [9, 15, 18], as the concentration of free holes in PbTe crystals (typically $P \simeq 3 \times 10^{18}$ cm^{-3} at $T = 77$ K) almost does not depend on the Mn content.

Implantation of Mn into PbTe epitaxial layers on BaF substrates leads to n-type conductivity of the layers, which is due to the presence of interstitial Pb [19].

In the present paper we tried to study the state of Mn ions in as-grown PbTe single crystals and possibilities to change their positions in the PbTe lattice by different treatments. Long-period 'thermal annealing' (in natural conditions at $T = 300$ K) was used. For another type of treatment laser annealing in the matrix transparency region was used, as it was earlier shown [7, 20] that such type of annealing leads to regulating of distribution both of native Pb and Eu ions in the PbTe lattice.

2. Samples and experimental procedures

PbTe : Mn single crystals, containing Mn in a solid phase $N_{Mn} \simeq 2 \times 10^{18}$–$1 \times 10^{20}$ cm^{-3} and obtained by Czochralsky technique, were used for investigation of EPR, electrical

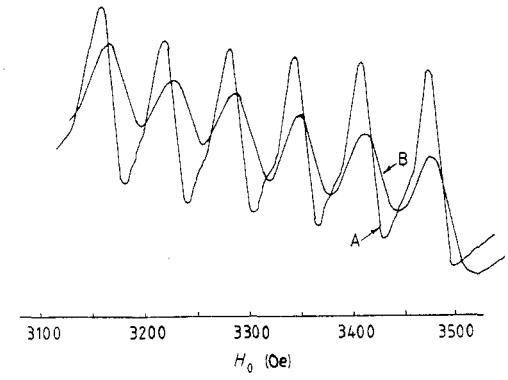

Figure 1. EPR spectra of a PbTe : Mn single crystal with Mn content $N_{Mn} \simeq 2 \times 10^{18}$ cm^{-3}. A—T = 77 K; B—T = 300 K.

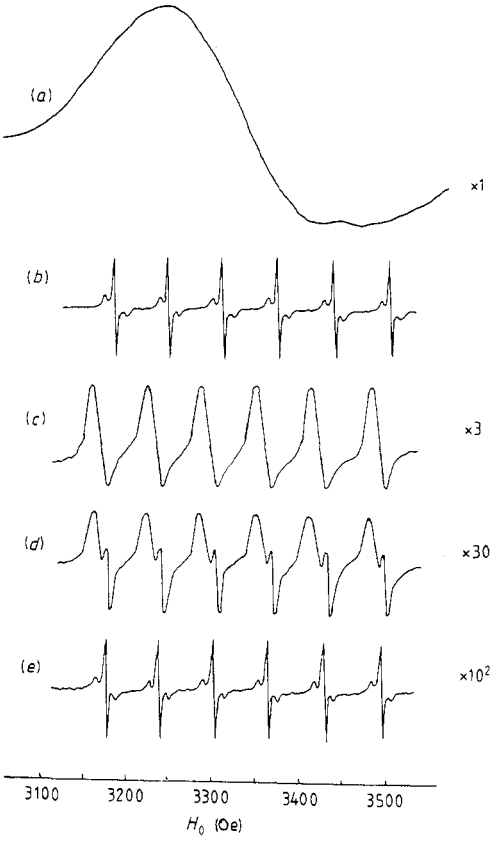

Figure 2. EPR spectra of PbTe : Mn single crystals: (*a*) in as-grown sample with $N_{Mn} = 2.2 \times 10^{19}$ cm^{-3}; (*b*) in the same sample after long-period (~3 years) 'annealing' in natural conditions; (*c*) after 10 h of laser treatment with $W \simeq 40$ W cm^{-2}; (*d*) after 20 h of laser treatment with $W \simeq 40$ W cm^{-2}; (*e*) after 20 h of laser treatment with $W \simeq 40$ W cm^{-2} in an external electric field $\boldsymbol{E}_{ex} \simeq 0.1$ V cm^{-1}. For each experiment $T = 20$ K. The figures beside the curves show the increase of the intensity of the EPR signals after laser treatment.

characteristics and optical transmission experiments. The manganese concentration was obtained by spectrochemical method. The X-band EPR measurements were performed at T = 4.2–300 K using a Varian E-12 spectrometer. Temperature dependences of the Hall coefficient and electrical conductivity were studied by the constant current standard procedure in the same temperature range on the same crystals as were used in the EPR experiments. Spectral dependences of the optical transmission of PbTe : Mn specimens

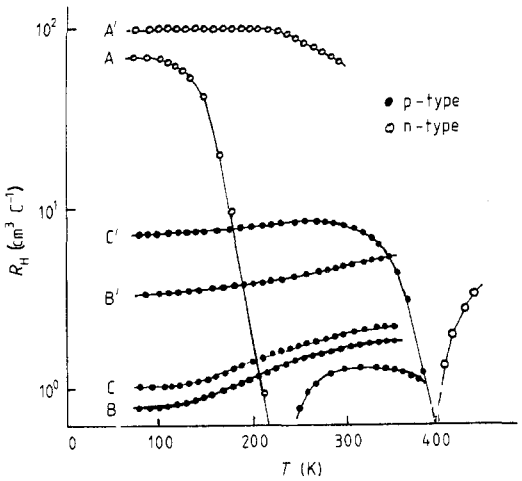

Figure 3. Temperature dependence of the Hall coefficient $R_H(T)$ of PbTe:Mn single crystals: in as-grown crystals (A, B, C), A—N_{Mn} 2.2×10^{19} cm^{-3} (n-type), B—$N_{Mn} = 1.9 \times 10^{19}$ cm^{-3} (p-type), C—$N_{Mn} = 2.2 \times 10^{19}$ cm^{-3} (p-type); after laser treatment with power density $W \simeq 20$ W cm^{-2} (A', B', C') for $t = 5$ h.

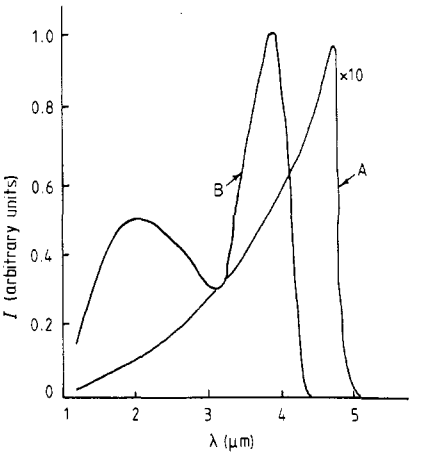

Figure 4. Spectral dependence of photosignals in undoped (A) and Mn-doped (B) PbTe single samples. $N_{Mn} \simeq 5 \times 10^{19}$ cm^{-3}. $T = 77$ K.

were studied at $T = 90$ and 300 K in the spectral range of wavelength $\lambda \simeq 4.5$–15 μm using grating spectrometer NKC-31.

3. Experimental details, and discussion of the results

3.1. Preliminary characteristics of the crystals

In the as-grown single PbTe : Mn crystals with Mn content $N_{Mn} \simeq 2 \times 10^{18}$ cm^{-3} as a rule six lines of HFS of Mn^{2+} in EPR spectra were observed at $T = 4.2$–300 K. These spectra are shown in figure 1 for $T = 77$ and 300 K. At $T = 77$ K the line shape of the EPR spectra and the parameters of spin-Hamiltonian (SH) obtained from the spectra almost do not depend on temperature. In crystals with Mn content $N_{Mn} \simeq 7 \times 10^{18}$ cm^{-3} one may observe six HFS line spectra or one broad line spectrum in the same temperature range. No relationship between the parts of the ingots from which the samples were cut and their EPR signal forms was found in crystals with such impurity concentration.

In the as-grown PbTe:Mn crystals with impurity content $N_{Mn} \geqslant 2 \times 10^{19}$ cm^{-3} one broad line of EPR spectra (figure 2(*a*)) was always observed. According to [17] from these Mn concentrations the Mn clustering starts in Czochralsky as-grown PbTe crystals.

As a rule, PbTe : Mn crystals were of p-type conductivity with the same concentration of carriers as in undoped crystals, $P_{77} \simeq 3 \times 10^{18}$ cm^{-3}, but in some crystals with $N_{Mn} \simeq 2 \times 10^{19}$ cm^{-3} n-type conductivity was observed at $T = 77$ K. The anomalous sign inversion of the Hall coefficient $R(T)$ in the range of temperatures $T \leqslant 230$ K (see figure 3) with a change of negative sign of R_H to positive was observed in such crystals. The reverse inversion of the Hall coefficient sign, as a result of the mobility ratio $b = M_n/M_p > 1$,

where M_n and M_p are the mobilities of electrons and holes respectively, is always observed in undoped PbTe crystals.

Independent of the conductivity type of such PbTe : Mn crystals, their carrier mobilities at $T = 77$ K, as a rule, did not exceed the value $M \simeq 2 \times 10^3$ cm^2 V^{-1} s^{-1}, that is, an order of magnitude lower than the value of M observed in undoped PbTe crystals with the same concentration of free carriers. The observed temperature dependences of $R_H(T)$ and the low values of M in the doped PbTe crystals obtained by the Czochralsky method seem to be due to the formation of impurity clusters or microfragments of the other crystal structure which are formed during lead telluride growth.

Potential barriers that appear at the interface of such defects within the PbTe matrix were found by the electron beam induced current (EBIC) method. These barriers effectively scatter the carriers, give rise to low values of M and lead to the anomalies of $R_H(T)$. Such defects at $T \lesssim 200$ K cause considerable photovoltaic effects observed in the crystals mentioned (the contacts being shielded from radiation). These defects are the reason for a cut-off wavelength shift of the photosignal towards shorter wavelengths in PbTe : Mn crystals, as compared to undoped PbTe samples (see figure 4). This is due to separation of photoexcited carriers by the barrier potentials in the bulk of the doped crystals [5].

3.2. Low-temperature long-period 'annealing'

PbTe : Mn single crystals ($N \gtrsim 7 \times 10^{18}$ cm^{-3}) in which EPR has been already studied (the EPR spectra of one of such samples with $N_{Mn} \simeq 2 \times 10^{19}$ cm^{-3} is shown in figure 2(*a*)), were subjected to long-period 'annealing' for a time $t \simeq 3$ years at $T = 300$ K (storage under natural conditions) and then EPR was studied in them again. After such 'annealing' the EPR spectra considerably changed. Six narrow lines of Mn^{2+} ions HFS with a halfwidth $\Delta H \simeq 6$ Oe appeared (figure 2(*b*)). Each of the six HFS lines had satellites on its sides with approximately 14 times less intensity (for both lines) than the HFS lines. From the position of the lines one can attribute these lines to the SHFS of $3d^5$ Mn^{2+} electrons, located in the PbTe metal sublattice points, due to their interaction with one or possibly more ligands of the first coordination sphere which are ^{125}Te or ^{123}Te ions having spin nuclei $I = 1/2$. 7.1% of ^{125}Te and 0.87% of ^{123}Te isotopes are contained in the tellurium that was used for growing the PbTe crystals.

Why the ratio 1 : 4 : 1 is not observed, as it should be in the case [14] when all the Mn^{2+} are in metal sublattice points, is not clear now. Instead approximately the ratio of the intensity lines from 1 : 28 : 1 to 1 : 14 : 1 was observed, which possibly shows that the Mn ions part is an interstitial incorporation. Intensities differing from the ratio 1 : 4 : 1 were obtained in [6] too for SHFS lines of Mn^{2+} EPR spectra in the PbTe lattice. At the microwave powers of klystron used (up to 1 mW) no saturation of SHFS and HFS lines was observed at the temperature of the experiments, $T = 20$ K. No angular dependences of SHFS lines were observed either.

In such crystals the following constants of SH for Mn^{2+} ions in a PbTe lattice with NaCl type symmetry (the point group O^h) at $T = 20$ K were obtained: $g = 1.9923 \pm 0.0005$; HFS constant $A = (59.6 \pm 0.2) \times 10^{-4}$ cm^{-1}; SHFS constant $a_{Te} = (15.38 \pm 0.2) \times 10^{-4}$ cm^{-1}. These parameters are close to those obtained in [14] for PbTe single crystals at $T = 4.2$ K: $g = 1.994 \pm 0.001$; $A = (61.4 \pm 0.1) \times 10^{-4}$ cm^{-1}; $a_{Te} = (15.35 \pm 0.1) \times 10^{-4}$ cm^{-1}, though the value of A is lower than in known papers. The value of g differs from that obtained in [6] for Mn-implanted PbTe films where the layers

are strained: $g = 1.9996 \pm 0.0003$. In this paper $A = (61.2 \pm 0.05) \times 10^{-4}\,\mathrm{cm}^{-1}$ and $a_{\mathrm{Te}} = (15.4 \pm 0.1) \times 10^{-4}\,\mathrm{cm}^{-1}$.

The surface layers of the crystals, subjected to long-period 'annealing', had n-type conductivity, as was determined from the sign of the thermo-electromotive force by means of the thermal probe method.

The gradual layer-by-layer chemical treatment of such long-period 'annealed' PbTe : Mn crystals in the etching agent Br_2 + HBr to a depth corresponding to the skin-layer depth ($d \simeq 30\ \mu$m), resulted in the gradual weakening of the intensity of HFS and SHFS lines. When etching PbTe : Mn crystals to a depth exceeding that pointed out (up to $h \sim 100\ \mu$m), the EPR spectrum with the HFS constant $A = 59.6 \times 10^{-4}\,\mathrm{cm}^{-1}$ and g-value $g = 1.9923$ completely disappeared and one broad line appeared in the EPR spectra. Then the EPR spectra were the same that were observed in the as-grown crystals with Mn content $N_{\mathrm{Mn}} \geqslant 2 \times 10^{19}\,\mathrm{cm}^{-3}$. After etching the crystals to a depth $d \geqslant 30\ \mu$m the crystal surface as a rule changed the type of conductivity to p-type.

Thus, long-period 'annealing' at 300 K leads to the same results as thermal treatment of PbTe : Mn-implanted films annealed at relatively low temperatures $T \leqslant 340$ °C [6] and this seems to be due to the dissolution of Mn-enriched inclusions at the outer parts of the PbTe : Mn crystals investigated.

3.3. Laser annealing

In [7, 20] it was shown that it is possible to use laser radiation in the transparency region of the IV–VI semiconductor matrix ($\hbar\omega < E_g$, where E_g is the band gap; $\hbar\omega = 0.118$ eV, CO_2-laser) in order to dissolve metal-rich inclusions. This effect was explained by the migration of metal atoms from inclusions into the lattice points of the metal sublattice. This migration leads to a change of the carrier concentration up to inversion of the conductivity type from p- to n-type as a result of compensation of metal vacancies which are two-fold charged acceptors. Under these conditions the mobility of carriers increases considerably. In particular it was shown [7] that the intensity of EPR lines in PbTe : Eu crystals increases up to 30 times after treatment by laser radiation.

The observed changes of electronic properties also preserve their character under the combined effect of laser radiation and externally applied electric field $\boldsymbol{E}_{\mathrm{ex}}$. But the changes of the carrier concentration proceed at considerably higher rates [21].

In order to investigate the influence of the position of Mn ions in the PbTe lattice on the doping properties, the effect of IR laser treatment was used in the matrix transparency region, both for the crystals in which the HFS and SHFS lines had been observed after long-period 'annealing' but after etching the EPR spectrum looked like that shown in figure 2(*a*), and for the other crystals, in which only a broad structureless EPR line was observed ($N_{\mathrm{Mn}} \geqslant 2 \times 10^{19}\,\mathrm{cm}^{-3}$). Also the laser treatment was used for the crystals in which six HFS spectra were observed ($N_{\mathrm{MN}} \simeq 2\text{–}7 \times 10^{18}\,\mathrm{cm}^{-3}$).

Irradiation of PbTe : Mn samples by CO_2-laser radiation results in a decrease in the concentration of holes (figure 5) in p-type crystals (up to inversion of the conductivity type at higher power densities of laser radiation) and an increase of the electron concentration in n-type crystals. The mobilities of free carriers considerably increased in laser treated samples (figure 5) but did not exceed $M \simeq 3 \times 10^4\,\mathrm{cm}^2\,\mathrm{V}^{-1}\,\mathrm{s}^{-1}$ at $T = 20$ K and $N_{\mathrm{Mn}} \geqslant 2 \times 10^{19}\,\mathrm{cm}^{-3}$. These M-values exclude the helicon propagation depth influence δ^* on the intensity of the EPR spectra as $\delta_0/\delta^* = \sqrt{2}\,M^{-3/2}(c/H)^{3/2}$. Here δ_0 is the skin depth. In order that $\delta^*/\delta_0 \geqslant 1$ then $M \geqslant 5 \times 10^4\,\mathrm{cm}^2\,\mathrm{V}^{-1}\,\mathrm{s}^{-1}$ at $H \simeq 3.3 \times 10^3$ Oe was used in the EPR experiments.

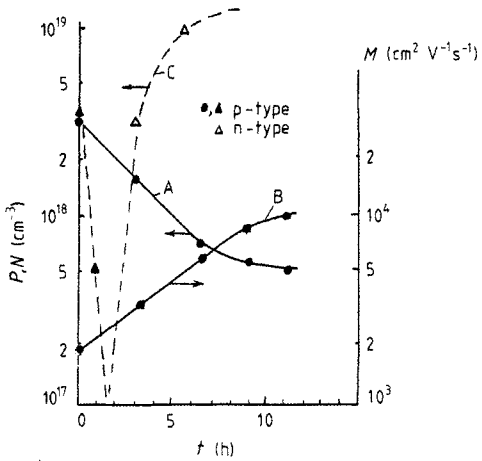

Figure 5. Dependence of free hole concentrations (A) and their mobilities (B) at $T = 77$ K on time of laser treatment in PbTe : Mn sample with $N_{Mn} \simeq 2 \times 10^{19}$ cm^{-3}. $W \simeq 40$ W cm^{-2}. C—dependence of free carrier concentration on time of laser treatment of PbTe : Mn sample placed in $E_{ex} \simeq 0.1$ V cm^{-1}, $W = 40$ W cm^{-2}. $T = 77$ K.

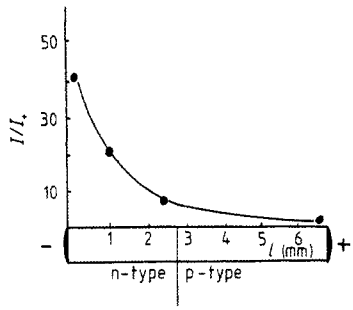

Figure 6. Distribution of the EPR signal intensity along one of the PbTe : Mn samples placed in a constant electric field and subjected to IR laser treatment. $N_{Mn} \simeq 2 \times 10^{19}$ cm^{-3}. $I_+/I_0 \simeq 3$, where I_+ and I_0 are the intensities of EPR signals in laser treated and untreated parts of the sample at the positive electrode respectively, referred to the unit volume.

The temperature dependences of $R_H(T)$ considerably change too (see figure 3) and become similar to those in undoped PbTe samples.

The observed changes of the electronic properties of PbTe : Mn crystals take place in the bulk as has been verified by studies of electrical characteristics of the samples under layer-by-layer etching up to the depth $h \simeq 100$ μm of each side of the samples, and also by studies of their optical transmission.

The optical absorption spectral dependences in p-PbTe : Mn crystals in the spectral range $\lambda \simeq 5$–15 μm at temperatures $T = 90$ and 300 K demonstrated an increase of the optical transmission of the samples from 1–2% for unirradiated samples to 15–20% for IR laser treated samples. This effect is associated with a decrease of the holes' concentration and an increase of their mobilities that lead to a decrease of the free carrier absorption. The maximum transmission is observed in the samples in which the change of conductivity type from p- to n-type is observed under the action of laser treatment. No additional absorption bands associated with the introduced Mn-impurity were detected in the spectral range $\lambda \simeq 5$–15 μm. The band gap E_g obtained at $T = 90$ and 300 K from the analysis of the optical absorption spectra at $N_{Mn} \lesssim 2 \times 10^{19}$ cm^{-3} correspond to the E_g-values in undoped PbTe samples.

The laser treatment of PbTe:Mn crystals resulted in considerable changes of EPR spectra. The single broad line observed before treatment (figure 2(a)) was transformed into a well resolved EPR spectrum consisting of six isotropic HFS lines with a half-width $H = 20$ Oe (like that shown in figure 2(c)). This spectrum at $T = 20$ K is characterized by the parameters: $g = 2.0033 \pm 0.0005$; $A = (59.9 \pm 0.2) \times 10^{-4}$ cm^{-1}. Similar parameters are observed in as-grown crystals with the lowest Mn content ($N_{Mn} \simeq 2 \times 10^{18}$ cm^{-3}). These parameters are close to those obtained in [10, 12].

For longer irradiation times the line intensities increased too (figure 2(*d*)) and a second group of isotropic lines with different halfwidth of the components appeared in the spectrum.

A further increase of the irradiation time resulted in a redistribution of EPR intensities in two groups of lines: the intensity of lines with a small halfwidth increased, while the intensity of the six HFS lines, which had appeared first and had larger halfwidth, decreased. But even under a relatively long time of IR-laser treatment ($t > 20$ h) lines with larger halfwidth were found in the EPR spectra.

When applying simultaneously to laser treated PbTe:Mn samples the weak external electric field ($\boldsymbol{E}_{ex} \| \boldsymbol{E}_l \| \langle 001 \rangle$, $\boldsymbol{E}_{ex} \simeq 0.01$–$0.1$ V cm^{-1}) where $\boldsymbol{E}_l$ is the electric field vector of the laser wave, a succession of EPR spectra transformation similar to that shown in figure 2(*a*), (*c*), (*d*) was observed, but for times an order of magnitude smaller than when the electric field was not applied. Under rather long-period ($t > 10$ h) simultaneous action of laser radiation and $\boldsymbol{E}_{ex}$ an EPR spectrum of Mn^{2+} ions was obtained which consisted only of six lines HFS with satellites of SHFS (figure 2(*e*)). This spectrum was characterized at $T = 20$ K by the parameters: $g = 1.9923 \pm 0.0005$; $A = (59.2 \pm 0.2) \times 10^{-4}$ cm^{-1}; $a_{Te} = 15.38 \times 10^{-4}$ cm^{-1}, which are the same as for the crystals long-period 'annealed' at $T = 300$ K.

After samples have been placed in an electric field and subjected to IR laser treatment the electrical characteristics of such crystals change faster too. The time needed for conversion of the conductivity type is rather short in that case and one can obtain n-type PbTe : Mn samples with high electron concentration (see figure 5).

For crystals with Mn content $N_{Mn} \lesssim 7 \times 10^{18}$ cm^{-3} in which six rather broad lines in EPR spectra were observed before laser treatment, after laser treatment in an external electric field at strengths like those pointed out in figure 1, a succession of EPR spectra like those shown in figures 2(*c*)–2(*e*) were observed.

All the peculiarities observed in the EPR spectra of PbTe : Mn crystals after IR laser treatment take place in the bulk of the samples as was tested by studying the EPR signals in the samples etched to a depth up to $h \simeq 100$ μm from each side or samples separated into several parts. After such operations the form of the curves did not change.

4. Directional migration of Mn^{2+} ions

In connection with the possibility the directional migration of Mn^{2+} ions in an external DC electric field $\boldsymbol{E}_{ex}$, one may expect a redistribution of Mn^{2+} ion concentration in the direction of $\boldsymbol{E}_{ex}$, applied parallel to the long sides of the specimens. After simultaneous application of $\boldsymbol{E}_{ex}$ and laser radiation to PbTe : Mn samples they were separated into several parts of equal length in which EPR as well as electrical characteristics were analysed.

Analysing the EPR spectra in different parts of the samples we observe that when passing from the parts near the positive electrode to those near the negative electrode, the EPR line intensity considerably increases (up to 40 times, see figure 6) while the halfwidth of each separate component decreases. In the parts of the crystals near the negative electrode the HFS line width was $\Delta H \simeq 6$ Oe, and SHFS lines were observed. The observed EPR spectra at $T = 20$ K were characterized by the same parameters as in crystals subjected to long-period 'annealing' under natural conditions.

Electrical characteristics of the parts of crystals subjected to simultaneous action of laser radiation and an external electric field varied as follows: the p-type conductivity

was observed in those parts of the crystal that were situated near the positive electrode (with the lowest EPR intensity); the conductivity type, when passing to the parts of the sample near the negative electrode changes to n-type (see figure 6). In the parts of the samples near the negative electrode the electron concentration reached $N_{77} \simeq 1.5 \times 10^{19}\,\mathrm{cm}^{-3}$, and this, according to the data of [20], corresponds to the saturation concentration of Te vacancies in PbTe, each of them being a two-fold ionized donor.

Thus, the Mn^{2+} ion migration to the negative electrode results in a filling of Pb vacancies (together with Pb^{2+} ions) in the metal sublattice (with a Pb vacancy concentration $N_{Pb} \simeq 5 \times 10^{19}\,\mathrm{cm}^{-3}$ [20] at the growth temperature). This results in the observation of HFS and SHFS lines of EPR spectra and the obtaining of limiting concentrations of electrons $N_{77} \simeq 1.5 \times 10^{19}\,\mathrm{cm}^{-3}$ (corresponding to a residual concentration of Te vacancies $N_{Te} \simeq 8 \times 10^{18}\,\mathrm{cm}^{-3}$).

So in the case when Mn^{2+} ions fill in the lead vacancies they act as pseudodonors, resulting in compensation of two holes from each lead vacancy. The electron concentration observed is due to Te–vacancies' donor action when every Te-vacancy is a doubly ionized donor.

In the as-grown PbTe:Mn samples with rather high manganese content ($N_{Mn} \geqslant 7 \times 10^{18}\,\mathrm{cm}^{-3}$) it seems that only a small part of the Mn ions fill the Pb vacancies and so cannot compensate for their acceptor influence ($N_{Pb} \simeq 5 \times 10^{19}\,\mathrm{cm}^{-3}$). So, not depending on Mn content in such a case, the Mn impurity behaves as a pseudo-amphoteric impurity.

5. Conclusion

From the analysis of the position, the form and the width of the EPR spectra and also the electrical characteristics both of as-grown and laser treated PbTe:Mn Czochralsky-grown samples with Mn content $N_{Mn} \simeq 2 \times 10^{18}$–$7 \times 10^{18}\,\mathrm{cm}^{-3}$, it can be assumed that a part of the Mn^{2+} ions in as-grown samples is interstitial and some part is in the metal sublattice points, which lead to six rather broad lines in the EPR spectra with effective g-factor $g = 2.0033$ and HFS constant $A = 59.9 \times 10^{-4}\,\mathrm{cm}^{-1}$.

At $N_{Mn} \geqslant 2 \times 10^{19}\,\mathrm{cm}^{-3}$ Mn atoms tend to form impurity-rich associations. This causes relatively bad electrical characteristics of the crystals and the availability of one broad EPR line of Mn^{2+} ions.

When creating the conditions that promote migration of Mn ions into PbTe metal sublattice points (long-period 'annealing' at natural conditions, laser treatment in the matrix transparency region) that are tested by the appearance of SHFS lines in the EPR spectra, the pseudodonor character of Mn impurity is apparent. This is due to compensation of the acceptor action of lead vacancies, which are two-fold charged acceptors, by Mn^{2+} ions (together with Pb^{2+} ions), and the appearance of donor action of residual Te-vacancies, which are two-fold charged donors.

So, the changing of the position of Mn impurities in the PbTe lattice considerably changes the electrical properties and EPR spectra of PbTe:Mn crystals that inevitably must change their semimagnetic properties.

Acknowledgment

The authors are grateful to S A Belokon for supplying the PbTe:Mn crystals.

References

[1] Kaidanov V I and Ravich Yu I 1985 *Usp. Phys. Nauk.* **145** 51
[2] Lischka K 1986 *Phys. Status Solidi* b 17
[3] Akimov B A, Brandt N B, Kurbanov K R *et al* 1983 *Phys. Tech. Poluprov.* **17** 1604 (Engl. Transl.: 1983 *Sov. Phys.–Semicond.* **17** 9)
[4] Gille P and Schenk M 1984 *Phys. Status Solidi* a **84** K121
[5] Belokon S A, Darchuck S D, Plyatsko S V *et al* 1988 *Izv. Akad. Nauk–Neorg. Mater.* **24** 1618
[6] Lettenmayr H, Jantsch W and Palmetshofer L 1987 *Solid State Commun.* **64** 1253
[7] Gromovoj Yu S, Plyatsko S V, Sizov F F and Darchuck S D 1989 *J. Phys.: Condens. Matter* **1** 6625
[8] Pifer J H 1967 *Phys. Rev.* **157** 272
[9] Toth G, Leloup J J and Rodot H 1970 *Phys. Rev.* B **1** 4573
[10] Inoue M, Yagi H, Muratani T and Tatsukawa T 1976 *J. Phys. Soc. Japan* **40** 458
[11] Tatsukawa T 1981 *J. Phys. Soc. Japan* **50** 515
[12] Hejwowski T and Subotowicz M 1981 *Phys. Status Solidi* b **106** 373
[13] Plyatsko S V, Gromovoj Yu S and Sizov F F 1985 *Kvantovaya Electron. (Kiev)* **29** 93
[14] Bartkowski M, Northcott P J and Reddoch A N 1986 *Phys. Rev.* B **34** 6506
[15] Andrianov D G, Belokon S A, Lakeenkov V M *et al* 1978 *Sov. Phys.–Semicond.* **12** 1322
[16] Escorne M, Mauger A and Triboulet R 1984 *Phys. Rev.* B **29** 6306
[17] Andrianov D G, Belokon S A, Lakeenkov V M *et al* 1980 *Phys. Tech. Poluprov.* **14** 175 (Engl. Transl.: 1980 *Sov. Phys.–Semicond.* **14** 1)
[18] Vanyarkho V G, Zlomanov V P, Dudkin L D *et al* 1970 *Izv. Akad. Nauk–Neorg. Mater.* **6** 1579
[19] Palmetshofer L, Wakolbinger B and Zinner E 1983 *Nucl. Instrum. Methods* **209/210** 725
[20] Sizov F F and Plyatsko S V 1988 *J. Cryst. Growth* **92** 571
[21] Plyatsko S V, Sizov F F and Darchuck S D 1988 *Mater. Lett.* **6** 116